Magnetic Resonance Imaging, Vol. 16, Nos. 5/6, pp. 605–607, 1998

Printed in the USA.
0730-725X/98 $19.00 + .00

PII S0730-725X(98)00044-7

● *Short Communication*

FLUID TRANSPORT IN GLASS BEADS PHANTOMS: SPATIAL VELOCITY MEASUREMENTS AND CONFIRMATION OF THE STOCHASTIC MODEL

M. BENCSIK,* B. ISSA,† M.A. AL-MUGHEIRY,‡ R.W. BOWTELL,* AND P. MANSFIELD*

*Magnetic Resonance Centre, Department of Physics, University of Nottingham, Nottingham, UK; †Centre for Magnetic Resonance Imaging, HRI, Hull, UK; and ‡Petroleum Development Oman, Muscat, Oman

A stochastic model of fluid flow in porous rocks has been previously developed to explain the measured distribution of local velocity. The theoretical predictions of this model agree well with experimental results obtained from the magnetic resonance imaging-based measurements of the spatial variation of velocity of water permeating through Bentheimer and Clashach sandstones. To further verify previous results, we have performed new velocity measurement experiments using an efficient velocity encoded π-echo planar imaging sequence on glass bead phantoms that exhibit more regular pore size distribution than rocks. The results show that velocity distributions in glass bead phantoms also exhibit Gaussian profiles and the linear relationship between the velocity variance and the mean velocity (the Mansfield-Issa equation).

Keywords: **π-echo planar imaging; Glass beads.**

INTRODUCTION

Previous measurements of the velocity distribution of water have been made in Bentheimer and Clashach sandstones. Our aim here was to repeat these experiments in a porous medium, where the pore size could be changed at convenience, and with homogeneous structure. Glass beads (JENCONS Ltd., Leighton Buzzard, UK) of different diameters were chosen. The π-echo planar imaging (PEPI) imaging sequence gives a satisfactory image and signal-to-noise ratio (SNR) as shown in Fig. 1.

EXPERIMENTAL DETAILS

Magnetic Resonance Imaging (MRI) Sequence

Spatially resolved measurements of the longitudinal component of the velocity of water flowing through glass bead phantoms were performed using a flow encoding sequence applied prior to the PEPI imaging sequence, as has been described in detail in previous publications.[2,3]

In this set of experiments, image artefacts were eliminated by using a large bird cage radiofrequency (rf) coil (diameter, 28 cm; length, 30 cm) but with lower SNR. More averaging was therefore necessary to achieve satisfactory SNR (400 acquisitions at the same flow rate were necessary for one map with a selected slice thickness of 10 mm, and a mean standard error on the measured phase of 10 degrees, corresponding to an SNR of 5.8).

Because of the large size of the rf coil, the shortest duration of the 180 rf pulses was 270 μs. The other parameters of the sequence used here are similar to those described elsewhere.[2]

New Sample

The sample holder used provides a cylindrical volume with a diameter of 7.6 cm and a length of 18 cm. Diffusers were placed at both the entry and the exit of the sample holder, so that a homogeneous velocity distribution would occur in the $[x, y]$ plane transverse to the main flow. Data shown here were achieved with packed glass beads of 5-mm diameter, with a selected slice thickness of 36 mm. Absolute values of the water flow rates driven through the beads were read from the display of the Gilson high pressure pump ($\pm$1% error), used for all the experiments.

Address correspondence to M. Bencsik, Magnetic Resonance Centre, Dept. of Physics, University of Nottingham, Nottingham, UK

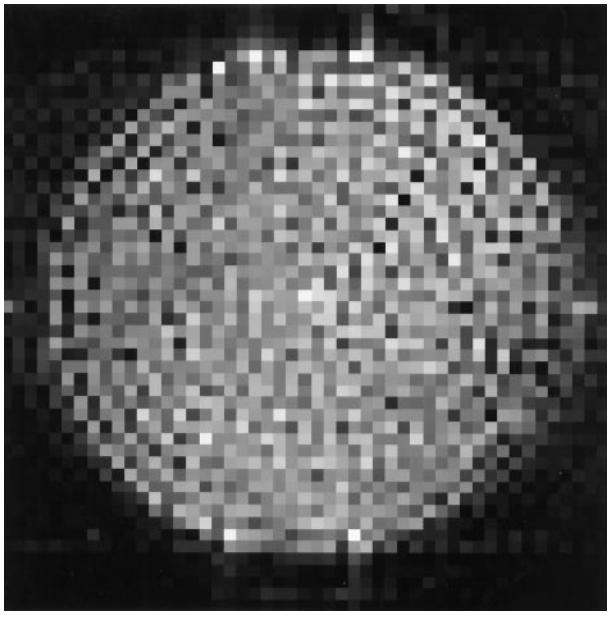

Fig. 1. Transverse section of 76-mm-diameter phantom containing water surrounding packed glass beads of 5-mm diameter. Slice thickness, 36 mm. Resolution, 1.8 × 1.8 mm^2.

THEORY

Both the Gaussian shape and the linear relationship between variance a^2 and mean velocity $\bar{v}$ of the longitudinal velocity distribution of water:

$$\frac{n}{\mathrm{N}} = \frac{100\delta v}{a\sqrt{2\pi}} \exp\left(-\left(\frac{(v-\bar{v})^2}{2a^2}\right)\right) \tag{1}$$

with

$$a^2 = \left(\frac{k'}{\rho}\right)\bar{v} \tag{2}$$

first observed in 1994 in different sandstones (Eqs. (4) and (5) in Ref. 4), are successfully explained by the hydrodynamic model of flow[2] of Mansfield and Issa, where ρ is the density of water, κ' is a constant related to the porous medium resistivity (Eqs. (7), (32d), and (33) in Ref. 2), (n/N) is the ratio of molecules of water with

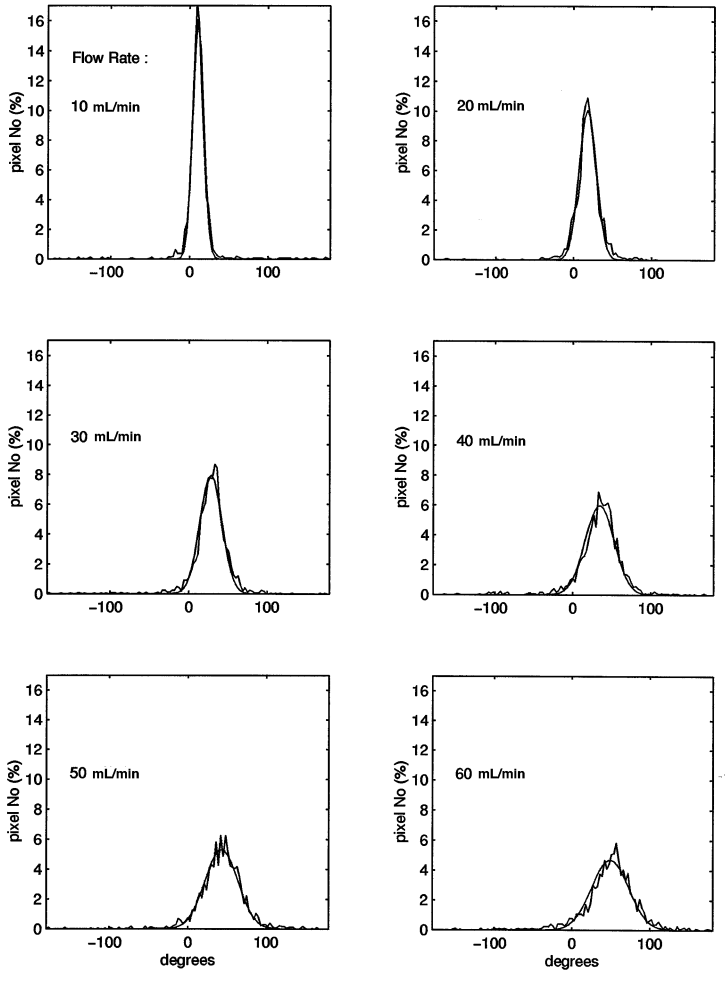

Fig. 2. Velocity-induced phase distributions of water flowing through glass beads (diameter, 5 mm). The full allowable phase range is displayed.

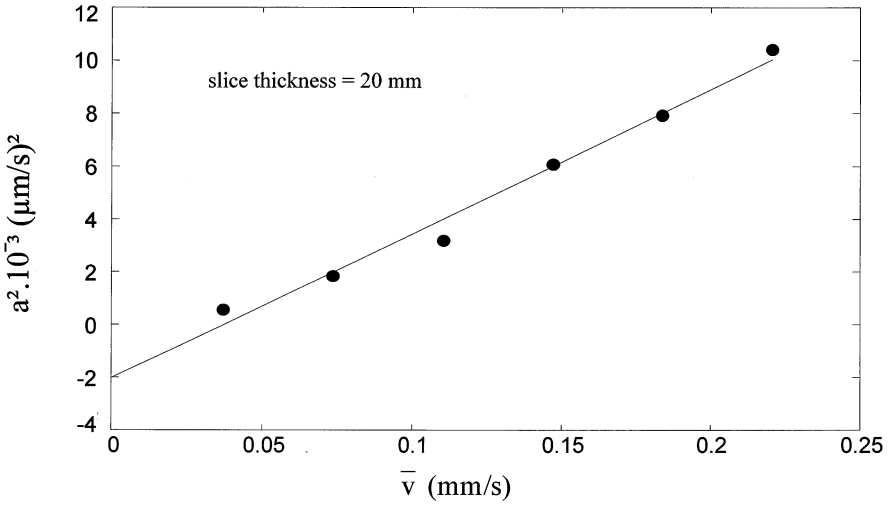

Fig. 3. Variance versus mean velocity in 5-mm-diameter glass beads.

velocity v, and δv is the flow interval used in plotting the data of Fig. 2.

EXPERIMENTAL RESULTS

Experimental Protocol

One experiment involved seven independent flow map acquisitions, with the mean velocity increasing from 0 to 0.22 mm/s in steps of 0.036 mm/s. The first phase map was used to eliminate eddy current-induced phase changes from the rest of the data. A phase histogram is formed from each phase map (Fig. 2).

The mean phase change of each flow map is plotted against the mean velocity measured from the known flow rate and sample diameter, and the best fit straight line gives the calibration of the flow encoding sequence (216° (±9%) per mm/s). The non-zero intercept of the straight line (2°) probably results from both imperfect compensation of eddy current-induced phase changes and, possibly, misevaluation of the velocity-induced mean phase change (only experimental points have been used for the evaluation of the best fit line as in Fig. 3). The linearity of the curve remains even at highest mean velocities, showing that phase wrap-around has been avoided throughout the experiment. This evaluation of the sensitivity of the experiment eventually allows us to display the fitted variance in (microns per second)^2 versus the mean velocity as shown in Fig. 3.

Small, negative values of the intercept of the best fit line could result from non-linearity of the curve at very low velocities. Thermal noise-induced broadening of the phase distributions displayed in Fig. 2 does not affect the estimate of the slope (79 (±7%) μm/s here), but adds a small positive offset to the curve. We have worked at keeping the mean standard error on the measurement of the phase change around 10°, although further work should allow us to decrease it to even lower value.

Evolution of the SNR during the Experiment

As the velocity distribution broadens with $\bar{v}$, the intravoxel phase distribution also broadens, resulting in pixel intensity decay. This decrease in the modulus of images results in an increase in the standard error of the measured phase along the experiment, from 7° to 12° in this particular set of data.

CONCLUSIONS

The linear relationship $a^2 = (k'/\rho)\,\bar{v}$ is shown to hold in a porous medium made up of packed glass beads of different sizes (100 μm to 10 mm). In future work, permeability in glass beads will be estimated with pressure drop measurement between the inlet and the outlet of the sample holder.

REFERENCES

1. Mansfield, P.; Issa, B. A microscopic model of fluid transport in porous rocks. Magn. Reson. Imaging 14:711–714; 1996.
2. Mansfield, P.; Issa, B. Fluid transport in porous rocks. Magn. Reson. Imaging A 122:137–148; 1996.
3. Guilfoyle, D.N.; Mansfield, P.; Packer, K. Fluid flow measurement in porous media by echo-planar imaging. J. Magn. Reson. 97:342–358; 1992.
4. Mansfield, P.; Issa, B. Studies of fluid transport in porous rocks by echo-planar MRI. Magn. Reson. Imaging 12:275–278; 1994.